Korean J. Chem. Eng., 35(1), 283-288 (2018)
DOI: 10.1007/s11814-017-0262-3

pISSN: 0256-1115
eISSN: 1975-7220

Synthesis of Ni promoted molybdenum dioxide nanoparticles using solvothermal cracking process for catalytic partial oxidation of *n*-dodecane

Kyungmin Im*, Hanseul Choi*, Kye Sang Yoo,†, and Jinsoo Kim*,†**

*Department of Chemical Engineering, Kyung Hee University, Yongin 17104, Korea
**Department of Chemical & Biomolecular Engineering, Seoul National University of Science and Technology, Seoul 01811, Korea
(*Received 18 August 2017 • accepted 20 September 2017*)

Abstract−Ni promoted MoO_2 nanoparticles were synthesized by combining spray pyrolysis and solvothermal cracking process. First, polycrystalline MoO_3 microparticles were prepared by spray pyrolysis at 600 °C. Then nano-sized Ni-MoO_2 particles were formed by solvothermal cracking process after adding Ni precursor, which disassembled polycrystalline MoO_3 microparticles into crystalline grains by thermal expansion and shattered them into Ni-MoO_2 nanoparticles by the subsequent solvothermal polyol reduction process. TPR profiles of Ni-MoO_2 nanoparticles presented the decrease of reducibility of MoO_2 with addition of Ni promoter. Catalytic partial oxidation of n-dodecane was conducted at various temperatures from 450 °C to 850 °C using Ni-MoO_2 nanoparticles and pure MoO_2 nanoparticles. H_2 yield of all the Ni-MoO_2 nanoparticles was higher than that of pure MoO_2 nanoparticles at 850 °C. Specially, 7 and 10 mol% Ni-MoO_2 nanoparticles showed desirable catalytic performance of ca. 60% of H_2 yield. This is mainly attributed to the existence of polymolybdate with addition of Ni and Ni^{2+} species partly located in the polymolybdate layer without formation of bulk Ni phase.

Keywords: Solvothermal Cracking, Ni, MoO_2 Nanoparticles, Polymolybdate, Partial Oxidation

INTRODUCTION

Molybdenum dioxide (MoO_2) has received great attention for its unusual metallic electrical conductivity related to mixed interatomic bonds and higher density states at the Fermi level [1]. These free electrons can enhance the catalytic activity of Mo^{+4} in MoO_2, contrasting the Mo^{+6} of MoO_3, where the valence electrons of the metal are bound to adjacent oxygen atoms [2]. Many researchers have thus studied MoO_2 as fuel reforming catalyst [1-3], alternative anode material for solid oxide fuel cells [4,5], and anode material for secondary lithium ion batteries [6,7]. Interestingly, MoO_2 has been studied as a hydrocarbon reforming catalyst such as jet-A fuel [1,3]. Unlike conventional Ni-based catalysts and commercial MoO_2 with low surface-area which was quickly deactivated by coking, MoO_2 nanoparticles showed a remarkably high fuel conversion and a desirable hydrogen yield with exceptional coking resistance [1,3,8].

Generally, MoO_2 has been prepared by reduction of MoO_3 using reducing gas at around 500 °C [9,10]. The reduction of MoO_3 to MoO_2 by reducing gas is relatively simple and commercially feasible, but this method has the disadvantage that the product particles are agglomerated easily. Moreover, MoO_2 with various structures was synthesized using high temperature deposition, electrochemical deposition, carbon nanotube template synthesis, and hydrothermal synthesis [11-13]. However, the product particle was still formed with relatively low surface area. Therefore, many researchers have used hydrothermal or solvothermal methods to directly produce MoO_2 with high specific surface area [1,9,14].

Recently, our research group developed the scalable synthesis method of MoO_2 nanoparticles through new solvothermal cracking process using the ultrasonic spray pyrolysis to produce polycrystalline MoO_3 microparticles and solvothermal reduction method to convert MoO_3 microparticles to pure MoO_2 nanoparticles [15]. Ni-promoted MoO_2 nanoparticles were prepared by the solvothermal cracking process to improve catalytic performance of MoO_2 nanoparticles [16]. The Ni-MoO_2 nanoparticles with various Ni concentrations were used as catalysts for partial oxidation of n-dodecane to investigate the effect of Ni promoting on the catalytic performance of MoO_2 nanoparticles.

EXPERIMENTAL

1. Synthesis of Ni/MoO_2 Nanoparticles

Initially, MoO_3 microparticles were prepared by ultrasonic spray pyrolysis as described elsewhere [17]. The precursor solution was prepared by adding 21.5 g of ammonium molybdate tetrahydrate ($(NH_4)6Mo_7O_{24}{\cdot}4H_2O$, 81-83%, Aldrich) in 200 ml of deionized water and then nebulized by a 1.7 MHz ultrasonic spray generator with six vibrators. The produced droplets were transferred into a quartz reactor heated to 600 °C. The residence time in the reactor was maintained at 2 seconds and the product particles were collected by a thimble filter.

Ni-MoO_2 nanoparticles were prepared by modified solvothermal cracking of MoO_3 microparticles synthesized via spray pyroly-

†To whom correspondence should be addressed.
E-mail: kyoo@snut.ac.kr, jkim21@khu.ac.kr
Copyright by The Korean Institute of Chemical Engineers.

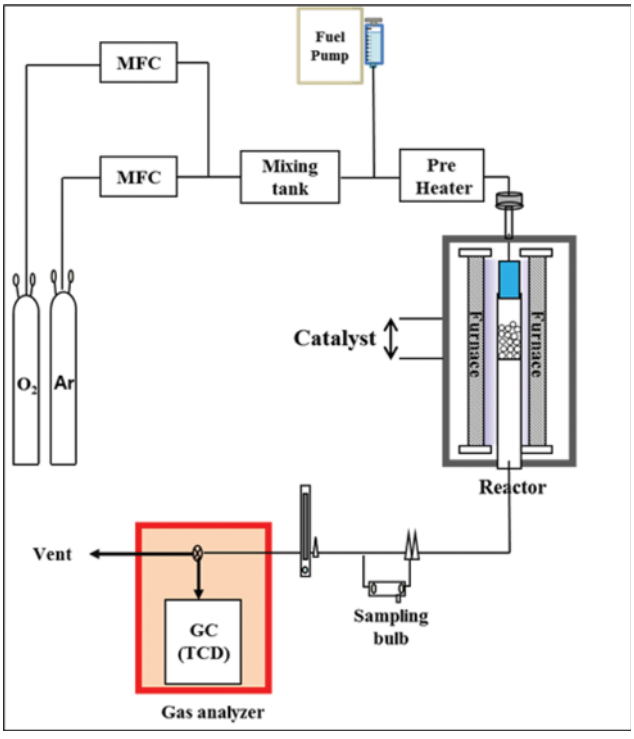

Fig. 1. Reactor apparatus for catalytic partial oxidation of *n*-dodecane.

sis. 1.2 g of as-synthesized MoO_3 microparticles were added in the solvent mixture of water and ethylene glycol (EG) with various volume ratios of 1 : 3, 1 : 1, and 3 : 3. Then nickel nitrate hexahydrate ($Ni(NO_3)_2 \cdot 6H_2O$, ≥97%, Aldrich) as nickel precursor was added into the MoO_3 suspension. After the mixed suspension was charged into the Teflon-lined autoclave, a solvothermal reaction was conducted at 210 °C for 12 h. After the solvothermal reaction, the product particles were obtained by centrifugation for 30 min and then washed in methanol three times. The final products were obtained after drying at 70 °C overnight. To investigate the effect of Ni concentration, various Ni/Mo molar ratios (3 mol%, 5 mol%, 7 mol%, and 10 mol%) were used for Ni-MoO_2 nanoparticles.

2. Characterizations

The crystal structure of Ni-MoO_2 nanoparticles was determined by using X-ray diffraction (XRD) using a Rigaku MAC-18XHF X-ray diffractometer equipped with a CuKα radiation source (λ= 1.54 Å) and measured at 2θ ranging from 20 to 80°. The morphology of Ni-MoO_2 nanoparticles and the distribution of the promoter (Ni) were investigated using field-emission scanning electron microscope (FE-SEM; Leo-Supra 55, Carl Zeiss STM, Germany). The interaction between Ni and MoO_2 was analyzed by high-resolution Raman spectroscopy (Renishaw inVia, UK).

Pure MoO_2 and Ni-MoO_2 particles were characterized by temperature-programmed reduction of hydrogen (H_2-TPR). For TPR analysis, the samples were reduced in H_2 environment at atmospheric pressure. During TPR process, the temperature of reactor was continuously heated to 850 °C with a heating rate of 2 °C/min. The H_2 consumption was measured by gas chromatography (6500GC System, Young Lin Instrument, Korea) with thermal conductivity detector (GC-TCD).

3. Catalytic Partial Oxidation of *n*-Dodecane

Ni-MoO_2 nanoparticles were used as catalysts for the partial oxidation of n-dodecane ($C_{12}H_{26}$), an alternative to diesel fuel. Reaction gas consisting of 20.5% oxygen and 79.5% argon was introduced into the preheater at 300 °C and mixed with the fuel at a flow rate of 0.5 ml/h. The oxygen to carbon (O_2/C) ratio during the test was maintained at 0.7 to maintain the molybdenum dioxide bulk phase. Space velocity (WHSV) was fixed at 5 h^{-1}. The catalysts were placed in a quartz reactor, sandwiched between two layers of quartz wool to maintain the bed position and prevent the catalysts from flowing out of the reactor with the gaseous products. Reactant gas mixture with n-dodecane was heated in the pre-heater before being introduced into the reactor. Flow rates of gas and liquid in the feed were controlled by a mass flow controller and syringe pump, respectively. After reaction, the products were analyzed by gas chromatography (GC-17A, Shimadzu, Japan) with a thermal conductivity detector. The detailed procedure can be found elsewhere [17].

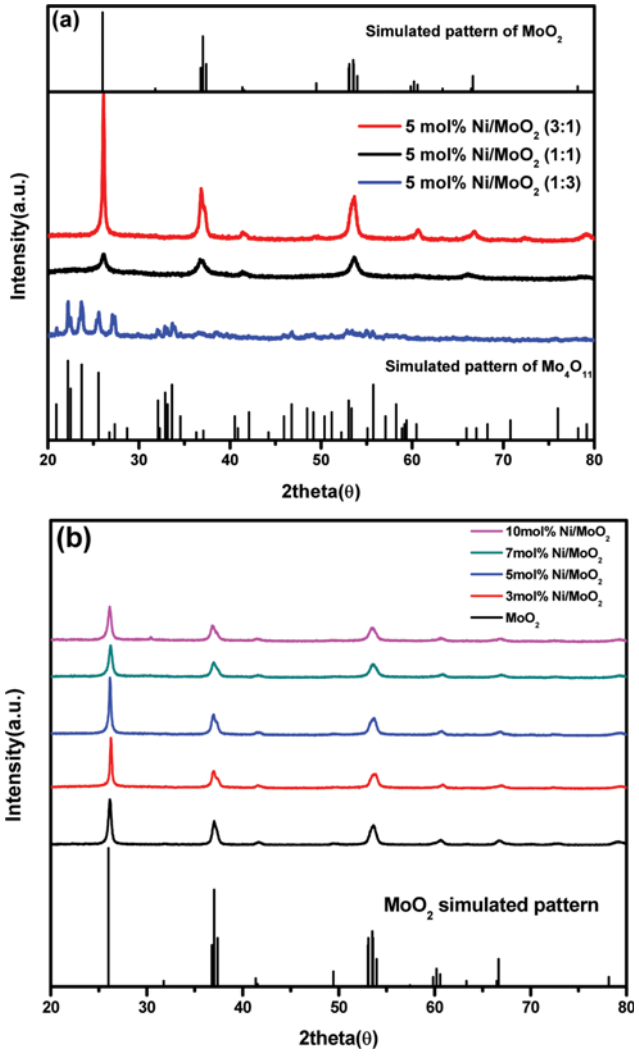

Fig. 2. XRD patterns of (a) 5 mol% of Ni/MoO_2 prepared in the various solvent compositions (H_2O : EG=1 : 3, 1 : 1, 3 : 1), and (b) 3, 5, 7, 10 mol% Ni/MoO_2 prepared in the solvent composition of H_2O : EG=3 : 1.

RESULTS AND DISCUSSION

1. Physicochemical Properties of Ni-MoO_2 Nanoparticles

MoO_2 nanoparticles containing various Ni concentrations were synthesized by solvothermal cracking method using MoO_3 microparticles prepared by spray pyrolysis. First, to determine the optimum volume ratio of water to EG for solvent, one of the most crucial synthesis conditions in the solvothermal cracking process, 5 mol% Ni-MoO_2 particles were synthesized in the various solvent mixture having the volume ratio of water to EG of 1 : 3, 1 : 1, and 3 : 1, under the identical solvothermal conditions (temperature: 210 °C, reaction time: 12 h). Fig. 2(a) shows XRD patterns of the product Ni-MoO_2 particles synthesized under various solvent compositions. The phase structures of the product particles were affected by the solvent compositions. When the ratio of water to EG was 1 : 3, Mo_4O_{11} phase (JCPDS: 05-0337) was formed obviously. Mo_4O_{11} phase is the intermediate phase for the reduction of MoO_3 into MoO_2 phase [15]. When the ratio of water to EG was 1 : 1, the crystal structure of product particle was transformed to pure MoO_2 phase (JCPDS: 32-0671). With further increasing water concentration to the ratio of water to EG=3 : 1, the crystallinity of MoO_2 phase increased without showing any detectable Ni species. As higher crystallinity is more preferable for catalytic activity, the ratio of water to EG was determined as 3 : 1 for further study.

Ni-MoO_2 nanoparticles with various Ni loading, 3, 5, 7 and 10 mol% were prepared under the identical conditions to investigate the effect of Ni content on their properties as catalysts for partial oxidation of n-dodecane. XRD patterns of the samples are shown in Fig. 2(b). All the particles except the sample with 10 mol% of Ni showed a comparable MoO_2 structure regardless of Ni concentration. 10 mol% Ni-MoO_2 showed a new small peak at 30.45°, which is mainly attributed to the appearance of $NiMoO_4$ phase [18]. The crystallite size of the samples was calculated by Scherrer equation and presented in Table 1. The crystallite sizes of 3 and 5 mol% Ni-MoO_2 nanoparticles were 36.2 nm and 35.8 nm, respectively, which were larger than that of MoO_2 (23.2 nm). This indicates that Ni promoter created nucleating centers that affect the growth of MoO_2 crystals [19]. For 7 and 10 mol% Ni-MoO_2 nanoparticles, however, the crystallite sizes decreased to 19.7 nm and 20.9 nm, respectively, which were smaller than that of pure MoO_2. It might be due to the fact that higher concentration of Ni promoters created a large number of nucleating centers that reached saturation state and these Ni promoters in lattice of MoO_2 induced more distorted structures [19].

Table 1. Crystallite size of MoO_2 and Ni-MoO_2 nanoparticles by Scherrer equation

Molar ratio of Ni/Mo	0	0.03	0.05	0.07	0.10
D (nm)	23.2	36.2	35.8	19.7	20.9

Morphology of Ni-MoO_2 nanoparticles was characterized using FE-SEM images as shown in Fig. 3. The 3 and 5 mol% Ni-MoO_2 showed a structure of aggregates, while the 7 and 10 mol% Ni-MoO_2 showed much smaller particles with very few aggregates. During the solvothermal cracking process, the mixture containing MoO_3 microparticles and Ni precursor was heated above the boiling point of the solvent mixture, which disassembled the polycrystalline MoO_3 particles to crystal grains along the grain boundary by thermal expansion [15]. These degraded crystal grains were further crushed to the nanoparticles by solvothermal cracking when MoO_3 was reduced to MoO_2 phase by EG. This crushing phenomenon is attributed to the crystal size difference between the MoO_3 phase and the MoO_2 phase [15]. Note that 7 mol% Ni-MoO_2 showed less aggregation than the other samples. The dispersion of Ni over MoO_2 was characterized by EDX dot mappings as illustrated in Fig. 4. The dot mapping images of Ni indicated that Ni promoters were

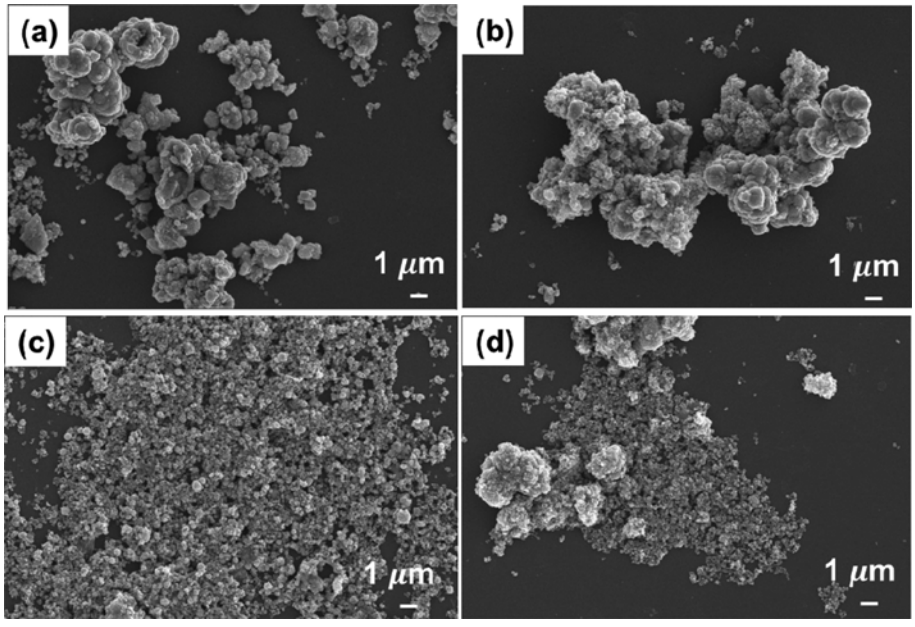

Fig. 3. FE-SEM images of Ni-MoO_2 nanoparticles with various Ni concentration: (a) 3 mol%, (b) 5 mol%, (c) 7 mol%, and (d) 10 mol%.

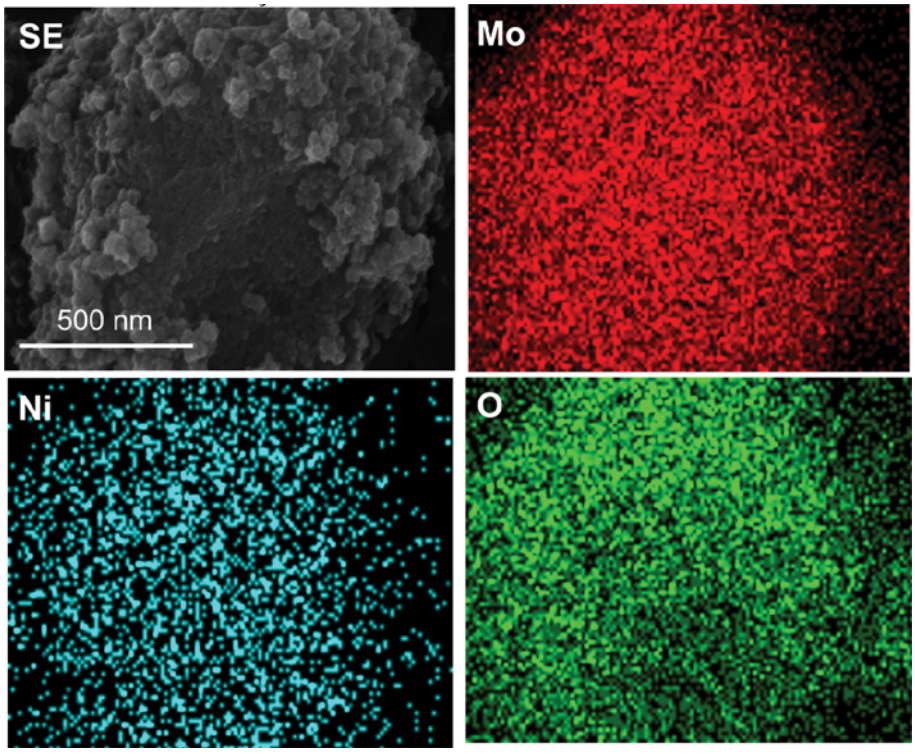

Fig. 4. Secondary electron image (a) and EDX dot mappings of Mo (b), Ni (c) and O (d) for 7 mol% Ni-MoO_2 nanoparticles.

well dispersed in the MoO_2 crystals.

H_2-TPR patterns of the samples were obtained to evaluate reduction behavior of Ni-MoO_2 nanoparticles and to study the interaction between Ni and MoO_2 as shown in Fig. 5. TPR profiles of pure MoO_2 indicated two major peaks at 330 °C and 810 °C, respectively. However, TPR profiles of all Ni-MoO_2 nanoparticles exhibited small peaks around 250-270 °C and large peaks around 770-810 °C. Both peaks in the low and high temperature regions of all the catalysts can be attributed to the reduction of the intermediate molybdenum phase on the MoO_2 phase and the respective MoO_2 reduction to the Mo metal [20-22]. The addition of Ni promoter caused the shifting of reduction temperature to a lower temperature [21,23].

2. Catalytic Performance of Ni-MoO_2 Nanoparticles

Catalytic performance of Ni-MoO_2 nanoparticles with various Ni concentrations was investigated with partial oxidation of n-dodecane between 450 °C and 850 °C. Weight-hourly-space-velocity (WHSV) and the volume ratio of O_2 to carbon were fixed at 5 hr^{-1} and 0.7, respectively. O_2/C ratio of 0.7 was selected because

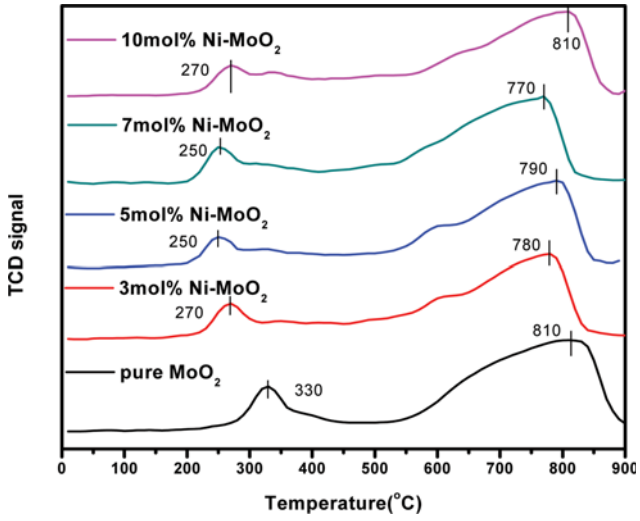

Fig. 5. H_2-TPR profiles of Ni-MoO_2 nanoparticles under 5 vol% H_2/Ar.

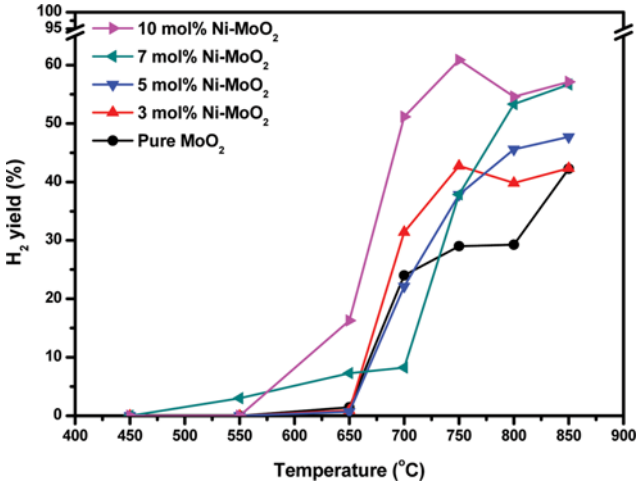

Fig. 6. Catalytic activity of Ni-MoO_2 nanoparticles toward partial oxidation of n-dodecane: H_2 yield.

MoO_2 phase was hardly transformed to Mo_2C phase during reaction [24]. The effect of reaction temperature on catalytic performance of Ni-MoO_2 nanoparticles with various Ni concentration is shown in Fig. 6. At reaction temperatures below 650 °C, all the catalysts showed negligible catalytic activities. However, at 650 °C, both 7 and 10 mol% Ni-MoO_2 particles started to show catalytic activities. When the reaction temperature increased above 650 °C, all the catalysts showed rapidly increased H_2 yields. At 850 °C, H_2 yield of pure MoO_2 was 42.27%. With increasing Ni concentration, H_2 yields increased to 42.33%, 47.70%, 56.68%, and 57.13%, respectively, for 3, 5, 7, and 10 mol% Ni-MoO_2. This result is attributed to the low reduction temperature of the Ni-MoO_2 nanoparticles as described in the TPR profile. Moreover, the light-off temperature of 7 and 10 mol% Ni-MoO_2 shifted to a lower value at 650 °C. This indicates that the redox cycle of MoO_2 based on the Martian-van Krevelen reaction mechanism is enhanced by the Ni promoter [1].

HR-Raman analysis was measured to identify the interaction between Ni and MoO_2 as illustrated in Fig. 7. All the samples showed one broad peak at 661-666 cm^{-1} and two sharp peaks at 819 cm^{-1} and 992-995 cm^{-1} that were related with MoO_2. In detail, 661 or 666 cm^{-1}, 819 cm^{-1} and 992 cm^{-1} were related with O-Mo-O stretch (υ_{as}), Mo=O stretch (υ_s), and Mo=O (υ_{as}) stretch, respectively [25]. Unlike the spectra of pure MoO_2 nanoparticles, the spectra of Ni-MoO_2 nanoparticles possessed small peaks at 949 cm^{-1} and 892 cm^{-1}. These peaks at 949 cm^{-1} and 892 cm^{-1} were stronger with increasing Ni loading. The peak at 949 cm^{-1} represents polymolybdate formed due to the addition of Ni^{2+} species. Dufresne et al. reported that Ni^{2+} species were partly located in the polymolybdate layer without formation of bulk $NiMoO_4$ phase [26]. Weak peaks of 5 to 10 mol% Ni-MoO_2 at 892 cm^{-1} were identified as $NiMoO_4$ phase. Therefore, a small amount of Ni impregnated in MoO_2 induced polymolybdate phase and further increasing of Ni loading strengthened the interaction between MoO_2 and Ni, resulting in formation of $NiMoO_4$ phase eventually [26,27]. From these results, it is obvious that Ni is well distributed over MoO_2 without formation of any bulk Ni phase. These Ni^{2+} species or $NiMoO_4$ phase played a significant role on improving their catalytic activity.

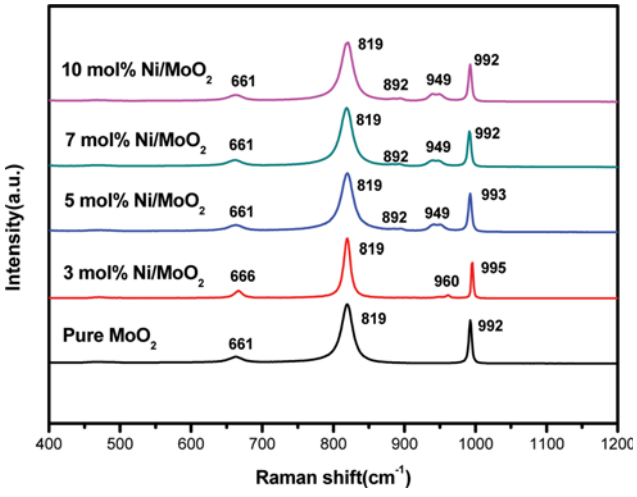

Fig. 7. HR-Raman spectra of pure MoO_2 and 3, 5, 7, 10 mol% Ni-MoO_2 nanoparticles.

CONCLUSION

Ni-MoO_2 nanoparticles were successfully synthesized by solvothermal cracking process combined with the ultrasonic spray pyrolysis. During the solvothermal cracking process, the polycrystalline MoO_3 microparticles prepared by spray pyrolysis were first disassembled into submicron particles, followed by the subsequent solvothermal polyol reduction into MoO_2 nanoparticles. The solvothermal cracking was mainly influenced by the ratio of water to EG in solvent to produce only pure MoO_2 phase. Most of 3 and 5 mol% Ni-MoO_2 nanoparticles were a structure of aggregates, while 7 and 10 mol% Ni-MoO_2 nanoparticles maintained smaller particles with few aggregates. These Ni-MoO_2 particles were used as the reforming catalysts for the partial oxidation of n-dodecane. Catalytic performance of Ni-MoO_2 particles outperformed that of pure MoO_2 regardless of Ni loading amount. Among the investigated Ni-MoO_2 particles, 7 and 10 mol% Ni-MoO_2 showed enhanced catalytic performances due to the existence of Ni^{2+} species or $NiMoO_4$ phase instead of bulky Ni phase.

ACKNOWLEDGEMENTS

This study was supported by the National Research Foundation of Korea (NRF) under the Ministry of Science, ICT & Future Planning (Basic Science Research Program (No. 2014R1A5A1009799).

REFERENCES

1. O. Marin-Flores, T. Turba, C. Ellefson, K. Wang, J. Breit, J. Ahn, M. G. Norton and S. Ha, *Appl. Catal. B: Environ.*, **98**(3), 186 (2010).
2. A. Katrib, P. Leflaive, L. Hilaire and G. Maire, *Catal. Lett.*, **38**(1), 95 (1996).
3. O. G. M. Flores and S. Ha, *Appl. Catal. A: Gen.*, **352**(1), 124 (2009).
4. B. W. Kwon, C. Ellefson, J. Breit, J. Kim, M. G. Norton and S. Ha, *J. Power Sources*, **243**, 203 (2013).
5. B. W. Kwon, S. Hu, O. Marin-Flores, M. G. Norton, J. Kim, L. Scudiero, J. Breit and S. Ha, *Energy Technol.*, **2**(5), 425 (2014).
6. Y. Shi, B. Guo, S. A. Corr, Q. Shi, Y. Hu, K. R. Heier, L. Chen, R. Seshadri and G. D. Stucky, *Nano Lett.*, **9**(12), 4215 (2009).
7. P. Han, W. Ma, S. Pang, Q. Kong, J. Yao, C. Bi and G. Cui, *J. Materials Chem. A*, **1**(19), 5949 (2013).
8. M. Matsumura and C. Hirai, *J. Chem. Eng. Japan*, **31**(5), 734 (1998).
9. C. A. Ellefson, O. Marin-Flores, S. Ha and M. G. Norton, *J. Mater. Sci.*, **47**(5), 2057 (2012).
10. A. F. Cotton, G. Wilkinson, M. Bochmann and C. A. Murillo, *Advanced inorganic chemistry*, Wiley (1999).
11. P. A. Spevack and N. S. McIntyre, *J. Phys. Chem.*, **97**(42), 11020 (1993).
12. J. Zhou, N. Xu, S. Deng, J. Chen, J. She and Z. Wang, *Adv. Mater*, **15**(21), 1835 (2003).
13. Y. Liang, Z. Yi, S. Yang, L. Zhou, J. Sun and Y. Zhou, *Solid State Ionics*, **177**(5), 501 (2006).
14. X. Chen, Z. Zhang, X. Li, C. Shi and X. Li, *Chem. Phys. Lett.*,

418(1), 105 (2006).
15. H. Choi, J. H. Heo, S. Ha, B. W. Kwon, S. P. Yoon, J. Han, W. Kim, S. H. Im and J. Kim, *Chem. Eng. J.*, **310**, 179 (2017).
16. H. Lee, G. S. Shin and Y. Kim, *Korean J. Chem. Eng.*, **32**(7), 1267 (2015).
17. H. Choi, D. Kim, S. P. Yoon, J. Han, S. Ha and J. Kim, *J. Anal. Appl. Pyrol.*, **112**, 276 (2015).
18. M. Liu, L. Kong, C. Lu, X. Ma, X. Li, Y. Luo and L. Kang, *J. Materials Chem. A*, **1**(4), 1380 (2013).
19. L. Xu and X. Li, *J. Cryst. Growth*, **312**(6), 851 (2010).
20. Q. He, O. Marin-Flores, S. Hu, L. Scudiero, S. Ha and M. G. Norton, *J. Nanoparticle Res.*, **16**(5), 2385 (2014).
21. L. Qu, W. Zhang, P. J. Kooyman and R. Prins, *J. Catal.*, **215**(1), 7 (2003).
22. P. Arnoldy, J. De Jonge and J. A. Moulijn, *J. Phys. Chem.*, **89**(21), 4517 (1985).
23. J. Chen, W. Li and R. Shen, *Korean J. Chem. Eng.*, **33**(2), 500 (2016).
24. O. Marin-Flores, T. Turba, J. Breit, M. G. Norton and S. Ha, *Appl. Catal. A: Gen.*, **381**(1), 18 (2010).
25. Q. He, O. Marin-Flores, S. Hu, L. Scudiero, S. Ha and M. G. Norton, *Scr. Mater.*, **100**, 55 (2015).
26. P. Dufresne, E. Payen, J. Grimblot and J. P. Bonnelle, *J. Phys. Chem.*, **85**(16), 2344 (1981).
27. E. Matsubara and K. Shinoda, *Japanese J. Appl. Phys.*, **38**(S1), 576 (1999).